PHYSICAL REVIEW A

GENERAL PHYSICS

THIRD SERIES, VOL. 6, NO. 5 NOVEMBER 1972

Single-Quantum Annihilation of Positrons by Screened K- and L-Shell Electrons*†

K. W. Broda‡ and W. R. Johnson
Department of Physics, University of Notre Dame, Notre Dame, Indiana 46556
(Received 3 January 1972)

Single-quantum annihilation of positrons in an atomic field is considered. Numerical calculations of the differential and total cross sections and the various polarization correlation functions are presented for the K and L shells of a range of elements from $Z=47$ to $Z=92$. The positron wave function is described by a partial-wave expansion in angular momentum eigenstates, and the interaction of the positron and bound electron with the radiation field is treated in lowest-order perturbation theory. Numerical programs are constructed for the solution of the radial part of the positron wave function and for the partial-wave phase shifts and normalization factors in an arbitrary non-Coulomb central potential, and for the evaluation of the differential and total cross sections. The effects of screening are included by using the bound-state wave functions and central potentials predicted by the relativistic Hartree-Fock-Slater atomic model. Screening corrections to the Coulomb K-shell total cross sections are found to be sizable for large atomic numbers and low positron energy, and the ratio of L- to K-shell total cross sections is found to be significant for heavy atoms. The angular distributions for this atomic potential exhibit the sharp forward peak predicted in previous work assuming a purely Coulombic potential.

I. INTRODUCTION

The existence of single-quantum annihilations (SQA) has been known for some time. Because of the difficulty of discriminating SQA radiation from background, experimental interest has been focused primarily on detection of the radiation[1,2] and measurement of total cross sections as functions of positron energy and atomic number.[3,4]

In order for SQA to occur, recoil momentum must be absorbed by the nucleus, so that the process is most probable for states having high charge densities near the nucleus. For this reason, and because screening effects were not thought to be important for the K shell, most previous theoretical calculations have been concerned only with K-shell annihilation in a Coulomb potential. After the early approximate calculations,[5–8] more recent work[9,10] has made use of relativistic Coulomb wave functions to evaluate K-shell total cross sections. K-shell differential cross sections for heavy atoms have been calculated recently by one of us,[11] and indicate a behavior in marked contrast to the earlier Born-approximation prediction.[8]

Although Bethe,[6] using the Born approximation, predicted that higher-shell contributions to the SQA cross section should be about 16% that of the K shell, little attempt has been made to evaluate the higher-shell contributions, except for the recent calculation for the L_I shell by Sheth and Swamy.[10] This is presumably due to the complexity of screening effects, which are expected to be important for these shells. Actually, it is found in this work that even for the K-shell, screening effects are important for low positron energy. Screening introduces two competing influences on SQA, one being the reduction of the effective nuclear charge, tending to reduce the cross section, the other being an inhibition of the Coulomb repulsion of the positron, tending to increase the cross section. In order to obtain a more reliable estimate of K-shell total cross sections than are predicted by a pure Coulomb potential, and to obtain a meaningful estimate of the relative importance of the screened L-shell contributions, K- and L-shell differential and total cross sections are calculated for several atoms and energies. This also serves as a check whether the sharp forward peak in the differential cross section for heavy atoms predicted earlier[11] is characteristic of only the Coulomb potential, or of any central potential. Screening is introduced by using the numerical

central potentials and bound-state wave functions predicted by the self-consistent, relativistic Hartree-Fock-Slater (RHFS) atomic model.

The positron's spin angular momentum is correlated with the polarization of the emitted photon. The correlation of the asymmetry of an unpolarized photon beam with the polarization of a positron beam in a direction perpendicular to the scattering plane has been discussed in a previous paper.[11] This correlation is extended to the L shell here. It is found here that there exists a correlation of positron helicity with left-right circular polarization of the emitted photon. Since for the K, L_{I}, and L_{II} shells the correlation is complete in the forward direction, where the peak of the angular distribution occurs for heavy atoms, it is suggested that SQA could be used as a technique to generate circularly polarized photon beams. The formulas for all nonzero correlations are given, and plots of the numerical results are reported for the correlations mentioned above.

Since SQA is a fundamental electromagnetic process, it is reasonable to expect that the degree of refinement of analysis should parallel that of, for example, the atomic photoeffect, in which higher shell contributions,[12] the effects of screening,[13,22] and polarization correlations[14] have been studied extensively. It is with this in mind that the present study was undertaken.

II. GENERAL FORMALISM

A. Differential Cross Section

The differential cross section for SQA is given by

$$\frac{d\sigma}{d\Omega}=\frac{\alpha}{2\pi}\frac{\omega E}{p}\left|T_{fi}\right|^2, \tag{1}$$

with

$$T_{fi}=\int d^3x\, v^{\dagger}_{\vec{p}\lambda}(\vec{x})\,\vec{\alpha}\cdot\vec{A}^{*}(\vec{x})\,u_B(\vec{x})\ . \tag{2}$$

In the amplitude T_{fi}, $v_{\vec{p}\lambda}(\vec{x})$, and $u_B(\vec{x})$ represent the four-component wave functions for the positron and bound-state electron, respectively. $\vec{A}(\vec{x})$ is the spatial part of the wave function for an emitted photon having energy-momentum four vector $k_\mu=(\vec{k},i\omega)$ (natural units are used throughout) and unit polarization vector $\hat{\epsilon}$:

$$\vec{A}(\vec{x})=\hat{\epsilon}\,e^{i\vec{k}\cdot\vec{r}} \tag{3}$$

and

$$\vec{\alpha}=\begin{pmatrix}0 & \vec{\sigma}\\ \vec{\sigma} & 0\end{pmatrix},$$

where σ_i are the 2×2 Pauli spin matrices. The momentum four vector of the positron is denoted by $p_\mu=(\vec{p},iE)$. The differential cross section in Eq. (1) will be summed over all magnetic substates of an atomic subshell, but the positron spin and photon polarization will be arbitrary.

B. Bound-State Wave Functions

The bound-state wave function $u_B(\vec{x})$ is described by the four-component spinor

$$u_{n_B\kappa_B m_B}=\begin{pmatrix} ig_{n_B\kappa_B}(r)\Omega_{\kappa_B m_B}(\hat{r})\\ f_{n_B\kappa_B}(r)\Omega_{-\kappa_B m_B}(\hat{r})\end{pmatrix}. \tag{4}$$

Here, n_B is the principal quantum number and κ_B, m_B define the angular momentum state. (The subscript B will denote bound-state quantum numbers).

The explicit form of $\Omega_{\kappa m}$ in terms of the Pauli spinors χ_λ is

$$\Omega_{\kappa m}(\hat{r})=\textstyle\sum_\lambda C(l\tfrac{1}{2}j;m-\lambda,\lambda)\,\chi_\lambda\,Y_l^{m-\lambda}(\hat{r})\ , \tag{5}$$

where κ is related to j and l by

$$\kappa=\mp(j+\tfrac{1}{2})\quad\text{for } j=l\pm\tfrac{1}{2}\ , \tag{6}$$

and where $C(l_1,l_2,l_3;m_1,m_2)$ is the Clebsch-Gordan coefficient according to the phase convention of Rose.[15] The function $u_{n_B\kappa_B m_B}$ is normalized so that

$$\int_0^\infty r^2(g^2_{n_B\kappa_B}+f^2_{n_B\kappa_B})\,dr=1\ , \tag{7}$$

and is a solution to the Dirac equation in a central potential $V(r)$:

$$[\vec{\alpha}\cdot\vec{p}+m\beta+V(r)]u_{n_B\kappa_B m_B}=E_B u_{n_B\kappa_B m_B}\ . \tag{8}$$

Equation (8) reduces to two coupled first-order differential equations in r:

$$\begin{aligned}&\frac{dg_\kappa}{dr}+\frac{(1+\kappa)g_\kappa}{r}+[E+m-V(r)]f_\kappa=0\ ,\\ &\frac{df_\kappa}{dr}+\frac{(1-\kappa)f_\kappa}{r}-[E-m-V(r)]g_\kappa=0\ .\end{aligned} \tag{9}$$

C. Positron Wave Functions

The wave function $v_{\vec{p}\nu}$ used to describe an incident positron of momentum $\vec{p}$ and spin projection ν in the rest frame, which asymptotically approaches a plane wave plus an outgoing spherical wave, is

$$v_{\vec{p}\nu}(\vec{r})=4\pi\sum_{\kappa m}(-1)^{\nu-1/2}(\Omega^{\dagger}_{\kappa m}(\hat{p})\,\chi_{-\nu})\,(-i)^{l-1}\times e^{-i\delta_\kappa}\begin{pmatrix} f_\kappa(r)\Omega_{-\kappa m}(\hat{r})\\ -ig_\kappa(r)\Omega_{\kappa m}(\hat{r})\end{pmatrix} \tag{10}$$

and is obtained from the corresponding partial-wave decomposition of a continuum electron with momentum $p_\mu=(\vec{p},iE)$ and spin ν by the familiar charge conjugation procedure.[16] If $V(r)$ is some arbitrary central potential, f_κ and g_κ of Eq. (10) are then radial functions for an electron described by $\vec{p}$ and ν, and are solutions to Eq. (9) with $V(r)$

replaced by $-V(r)$. Likewise, the phase shifts δ'_κ are those for an electron in a potential $-V(r)$, and are given by

$$\delta'_\kappa = \delta_\kappa + \tfrac{1}{2}(l+1)\pi\,, \qquad \delta'_\kappa = 0 \text{ for } V(r)=0\,. \tag{11}$$

The normalization of the radial functions g_κ and f_κ are such that their asymptotic forms are given by

$$\begin{aligned} g_\kappa(pr) &\to \left(\frac{E+m}{2E}\right)^{1/2} \frac{\cos(pr+\delta'_\kappa)}{pr}\,, \quad pr\to\infty \\ f_\kappa(pr) &\to \left(\frac{E-m}{2E}\right)^{1/2} \frac{\sin(pr+\delta'_\kappa)}{pr}\,, \quad pr\to\infty\,. \end{aligned} \tag{12}$$

D. Potentials

The central potentials used in the solution of Eq. (9) are those furnished by the RHFS atomic model,[17,18] in which electron-electron interactions are treated in lowest-order perturbation theory. If retardation effects are neglected, the potentials are given in the form

$$V_{\rm HFS} = -(\alpha Z/r) + V^D(r) - \overline{V}^E(r)\,. \tag{13}$$

Here $\overline{V}^E$ is the average of the exchange-interaction term over all filled subshells according to the technique of Slater,[19] and

$$\begin{aligned} V^D(r) &= \frac{\alpha}{r}\left(\int_0^r n(r')\,dr' + r\int_r^\infty \frac{dr' n(r')}{r'}\right), \\ \overline{V}_E &= 3\alpha\left(\frac{3}{32\pi^2}\frac{n(r)}{r^2}\right)^{1/3}, \\ n(r) &= \textstyle\sum_\kappa (2j_\kappa+1) r^2 (g_\kappa^2 + f_\kappa^2)\,, \end{aligned} \tag{14}$$

where the summation in the last equation is over all occupied subshells.

E. Radiation Field

The radiation field in Eq. (2) is treated in the form of an expansion in electric and magnetic multipoles:

$$\vec{A}(\vec{r}) = \sum_{\lambda=0}^{1} \sum_{JM} C^\lambda_{JM} A^\lambda_{JM}(\hat{r}) \tag{15}$$

with

$$C^\lambda_{JM} = 4\pi i^{J-\lambda} Y^\lambda_{JM}(\hat{k})^\dagger \cdot \hat{\epsilon}\,, \tag{16}$$

$$A^{(0)}_{JM} = j_J(\omega r)\, Y_{JJM}(\hat{r})\,, \tag{17a}$$

$$A^{(1)}_{JM} = j_{J-1}(\omega r)\left(\frac{J+1}{2J+1}\right)^{1/2} Y_{J,J-1,M}(\hat{r}) - j_{J+1}(\omega r)\left(\frac{J}{2J+1}\right)^{1/2} Y_{J,J+1,M}(\hat{r})\,. \tag{17b}$$

The functions $Y_{JLM}(\hat{r})$ are the vector spherical harmonics as defined by Akhiezer and Berestetskii.[20] In terms of angular momentum coupling coefficients, the Y_{JLM} have the form

$$Y_{JLM}(\hat{r}) = \sum_{\mu=-1}^{+1} C(L1J; M-\mu, \mu)\, Y_L^{M-\mu}(\hat{r})\,\chi_\mu\,, \tag{18}$$

where the χ_μ are unit vectors in a spherical basis.[20] $j_J(\omega r)$ is the spherical Bessel function of order J. The $Y^{(\lambda)}_{JM}(\hat{r})$ are constructed as linear combinations of $Y_{JJ'M}(\hat{r})$ in such a way that they are transverse for $\lambda = 0, 1$. The $C^{(0,1)}_{JM}$ terms are classified as magnetic and electric multipoles, respectively.

F. Form of Matrix Element

With the radiation field expressed in the form of Eq. (15), the matrix element of Eq. (2) is written as a sum of multipole contributions:

$$\begin{aligned} T_{fi} &= \sum_{JM\lambda} T^{(\lambda)}_{JM}\,, \\ T^{(\lambda)*}_{JM} &= C^{(\lambda)}_{JM} \int d^3x\, u^\dagger_{\kappa_B m_B}(\vec{x})\, \vec{\alpha}\cdot A^{(\lambda)}_{JM}(\vec{x})\, v_{\mathfrak{F}\lambda}(\vec{x})\,. \end{aligned} \tag{19}$$

Defining the radial integrals

$$\begin{aligned} I_{\kappa\kappa_B J} &= e^{i\delta'_\kappa} \int_0^\infty r^2\, dr\, f_\kappa(r) f_{\kappa_B}(r) j_J(\omega r)\,, \\ K_{\kappa\kappa_B J} &= e^{i\delta'_\kappa} \int_0^\infty r^2\, dr\, g_\kappa(r) g_{\kappa_B}(r) j_J(\omega r)\,, \end{aligned} \tag{20}$$

where the partial-wave phase shifts δ'_κ and the functions f_κ, g_κ are those of expansion (10), and defining the linear combinations

$$R^{(0)}_{\kappa\kappa_B J} = I_{\kappa\kappa_B J} + K_{\kappa\kappa_B J}\,, \tag{21a}$$

$$\begin{aligned} R^{(1)}_{\kappa\kappa_B J} = \frac{1}{2J+1}\,\frac{1}{\kappa-\kappa_B}\,\big[&(J+1)(J+\kappa+\kappa_B) I_{\kappa\kappa_B J} \\ &+ J(J+1-\kappa-\kappa_B) I_{\kappa,\kappa_B,J+1} \\ &- (J+1)(J-\kappa-\kappa_B) K_{\kappa,\kappa_B,J-1} \\ &- J(J+1+\kappa+\kappa_B) K_{\kappa,\kappa_B,J+1}\big]\,, \end{aligned} \tag{21b}$$

the various multipole contributions of the matrix element (19) become

$$\begin{aligned} T^{(\lambda)}_{JM} = 4\pi(-1)^{s-1/2+\lambda}\{1/[J(J+1)]\}^{1/2} C^{(\lambda)*}_{JM} \\ \times \sum_{\kappa m} \chi^\dagger_{-s}\, \Omega_{\kappa m}(\hat{p})\, i^{l-1} \\ \times (\kappa-\kappa_B) I_{\kappa_B m_B;\,\kappa_1 m;\,JM} R^{(\lambda)}_{\kappa\kappa_B J}\,, \end{aligned} \tag{22}$$

with $\kappa_1 = +\kappa, -\kappa$ for $\lambda = 0, 1$, and the factor $I_{\kappa_1 m_1;\kappa m;\,JM}$ given by

$$\begin{aligned} I_{\kappa_1 m_1;\kappa m;\,JM} = (-1)^{J+j-j_1}\left(\frac{(2J+1)(2j+1)}{4\pi(2j_1+1)}\right)^{1/2} \\ \times \Pi_{lJl_1} C(jJj_1;\tfrac{1}{2}0) C(jJj_1; mMm_1)\,, \end{aligned} \tag{23}$$

where $\Pi_{lJl_1} = 1, 0$ for $(l+J+l_1)$ even or odd, respectively.

The matrix element T_{fi} is most easily reduced in a coordinate system in which $\vec{k}$ defines the polar

z axis and $\vec{k}\times\vec{p}$ the y axis, so that the photon polarization unit vector has the expansion

$$\hat{\epsilon}=e^{(1)}\chi_1+e^{(-1)}\chi_{-1}\ , \tag{24}$$

with $|e^{(1)}|^2+|e^{(-1)}|^2=1$, $e^{(\pm1)}$ being the contravariant components of $\hat{\epsilon}$ in the spherical basis defined by χ_0, $\chi_{\pm1}$.[20] The amplitude T_{fi} for a given bound state κ_B, m_B is then given by

$$(T_{fi})_{\kappa_B,m_B}=(-1)^{s-1/2}\,\chi^{\dagger}_{-s}\begin{bmatrix}G_+e^{(1)*}-G_-e^{(-1)*}\\ F_+e^{(1)*}-F_-e^{(-1)*}\end{bmatrix}_{\kappa_B m_B}\ , \tag{25}$$

with

$$\begin{pmatrix}G_\pm\\ F_\pm\end{pmatrix}_{\kappa_B,m_B}=\begin{pmatrix}M^{(0)}_\pm\pm M^{(1)}_\pm\\ N^{(0)}_\pm\pm N^{(1)}_\pm\end{pmatrix}_{\kappa_B,m_B}\ , \tag{26}$$

$$\begin{pmatrix}M^{(\lambda)}_\pm\\ N^{(\lambda)}_\pm\end{pmatrix}_{\kappa_B,m_B}=4\pi\sum_J\frac{2J+1}{[J(J+1)]^{1/2}}\frac{1}{[2j_B+1]^{1/2}}\,i^{J+\lambda}C(J1J;01)\sum_\kappa i^{l-1}(\kappa-\kappa_B)$$
$$\times(-1)^{j+1-j_B-\lambda}(2j+1)^{1/2}C(jJj_B;\tfrac{1}{2}0)R^{(\lambda)}_{\kappa\kappa_B J}\,\Pi_{l_\lambda J l_B}\begin{pmatrix}\mathfrak{M}_\pm(\kappa,J)\\ \mathfrak{N}_\pm(\kappa,J)\end{pmatrix}\ . \tag{27}$$

Here, $l_0=l(\kappa)$, $l_1=l'(\kappa)=l(\kappa)-\mathrm{sign}(\kappa)$. Also,

$$\begin{pmatrix}\mathfrak{M}_\pm(\kappa,J)\\ \mathfrak{N}_\pm(\kappa,J)\end{pmatrix}_{\kappa_B,m_B}=C(jJj_B;m_B\mp1;\pm1)\begin{pmatrix}C(l\tfrac{1}{2}j;m_B-\tfrac{1}{2}\pm1,\tfrac{1}{2})Y_l(\hat{p})^{m_B-1/2\pm1}\\ C(l\tfrac{1}{2}j;m_B+\tfrac{1}{2}\mp1,-\tfrac{1}{2})Y_l(\hat{p})^{m_B+1/2\mp1}\end{pmatrix}\ . \tag{28}$$

Equations (26)–(28) define the amplitudes $G_\pm$ and $F_\pm$ in terms of radial integrals $R^{(\lambda)}_{\kappa\kappa_B J}$ and spherical harmonics.

G. Polarization Correlations

The polarization properties of the emitted photon in SQA can be described completely by the polarization density matrix ρ:

$$\rho_{\mu\nu}=a_\mu a^*_\nu\ ,\quad \mu=1,2 \tag{29}$$

where a_μ are the expansion coefficients for the unit polarization vector $\hat{\epsilon}$ subject to the normalization requirement $|a_1|^2+|a_2|^2=1$. If $\hat{\epsilon}$ is expanded in the spherical basis of Eq. (24), $a_1=e^{(1)}$ and $a_2=e^{(-1)}$. The matrix ρ can be expressed in terms of the familiar Stokes parameters ξ_i:

$$\rho=\tfrac{1}{2}(1+\sum_{i=1}^{3}\xi_i\sigma_i), \tag{30}$$

where σ_i are the Pauli spin matrices, and ξ_i are given by

$$\xi_j=\mathrm{Tr}\sigma_j\rho\ .$$

Since it can be shown that a photon that is completely right (left) circularly polarized is described by a polarization vector for which $|e^{(+1)}|^2=1$, ($|e^{(-1)}|^2=1$),[20] the quantity $\xi_3=|e^{(+1)}|^2-|e^{(-1)}|^2$ completely defines the left (right) circular polarization of the emitted photon. It is also possible to show that ξ_1 is a measure of the degree of transverse polarization along some appropriately chosen axis, and that ξ_2 is a measure of the degree of polarization along an axis forming a 45° angle with the axis defined by ξ_1.[20]

In terms of the Stokes parameters, the differential cross section for SQA can be put into the form used by Pratt *et al.*[14] in their study of the atomic photoeffect:

$$\frac{d\sigma}{d\Omega}=\sigma_0\,\tfrac{1}{2}\sum_{i,j=0}^{3}B_{ij}\xi_i\eta_j\ , \tag{31}$$

with $\xi_0=\eta_0=1$, and the η_j are the components of the positron spin in a coordinate system in which $\vec{p}$ defines the z axis and $\vec{k}\times\vec{p}$ the y axis.

The quantity of interest in this paper is the differential cross section for annihilation with all bound electrons in a filled subshell. Making use of the symmetry relations for the amplitudes $G_\pm$, $F_\pm$:

$$G_\pm(-m_B)=(-1)^{m_B+1/2}(\kappa_B/|\kappa_B|)F_\mp(m_B)\ ,$$
$$F_\pm(-m_B)=(-1)^{m_B-1/2}(\kappa_B/|\kappa_B|)G_\mp(m_B)\ , \tag{32}$$

the SQA differential cross section is given by Eq. (31), and

$$\sigma_0=\alpha E\omega/\pi p\ ,$$

$$B_{00}=\sum_{m_B>0}(|G_+|^2+|F_+|^2+|G_-|^2+|F_-|^2)_{m_B,\kappa_B}\ ,$$

$$B_{02}=-2\,\mathrm{Im}\sum_{m_B>0}(G_+F^*_+ + G_-F^*_-)_{m_B,\kappa_B}\ ,$$

$$B_{10}=-2\,\mathrm{Re}\sum_{m_B>0}(G_+G^*_- + F_+F^*_-)_{m_B,\kappa_B}\ ,$$

$$B_{12}=2\,\mathrm{Im}\sum_{m_B>0}(F_+G_-^*-G_+F_-^*)_{m_B,\kappa_B}\ ,$$

$$B_{21}=2\cos\theta\,\mathrm{Im}\sum_{m_B>0}(F_-G_+^*+G_-F_+^*)_{m_B,\kappa_B}$$
$$-2\sin\theta\,\mathrm{Im}\sum_{m_B>0}(F_+F_-^*-G_+G_-^*)_{m_B,\kappa_B}\ , \qquad (33)$$

$$B_{23}=2\sin\theta\,\mathrm{Im}\sum_{m_B>0}(F_-G_+^*+G_-F_+^*)_{m_B,\kappa_B}$$
$$+2\cos\theta\,\mathrm{Im}\sum_{m_B>0}(F_+F_-^*-G_+G_-^*)_{m_B,\kappa_B}\ ,$$

$$B_{31}=2\cos\theta\,\mathrm{Re}\sum_{m_B>0}(G_-F_-^*-G_+F_+^*)_{m_B,\kappa_B}$$
$$-\sin\theta\sum_{m_B>0}(|G_-|^2+|F_+|^2-|F_-|^2-|G_+|^2)_{m_B,\kappa_B}\ ,$$

$$B_{33}=2\sin\theta\,\mathrm{Re}\sum_{m_B>0}(G_-F_-^*-G_+F_+^*)_{m_B,\kappa_B}$$
$$+\cos\theta\sum_{m_B>0}(|G_-|^2+|F_+|^2-|F_-|^2-|G_+|^2)_{m_B,\kappa_B}\ .$$

Here, θ is the angle formed by $\vec{k}$ and $\vec{p}$. All other correlation functions are zero owing to the symmetry relations (32). Alternatively, the differential cross section can be written as

$$\frac{d\sigma}{d\Omega}=\left(\frac{d\sigma}{d\Omega}\right)_{\mathrm{unpol}}\frac{1}{2}\sum_{i,j}C_{ij}\xi_i\eta_j\ , \qquad (34)$$

with $C_{ij}=B_{ij}/B_{00}$. The C_{ij} have the convenient property that $-1\le C_{ij}\le 1$. The differential cross section for unpolarized positron and photon beams is given by $(d\sigma/d\Omega)_{\mathrm{unpol}}=\sigma_0 B_{00}$.

The total cross sections for unpolarized positron beams annihilating to give rise to unpolarized photon beams are given by the simple expression

$$\sigma=\frac{8\pi\,\alpha E\Omega}{p}\sum_J\frac{2J+1}{J(J+1)}\sum_\kappa(2l+1)C^2(l\,\tfrac{1}{2}j\,;0\,\tfrac{1}{2})(\kappa-\kappa_B)^2$$
$$\times C^2(jJj_B\,;\tfrac{1}{2}0)(|R^{(0)}_{\kappa\kappa_B J}|^2\Pi_{lJl_B}+|R^{(1)}_{\kappa\kappa_B J}|^2\Pi_{l'Jl_B})\ . \qquad (35)$$

III. NUMERICAL METHODS

The calculation of the differential and total cross sections, as well as all polarization correlation effects, is essentially complete once the radial integrals $I_{\kappa\kappa_B J}$ and $K_{\kappa\kappa_B J}$ have been obtained. Because the potentials are not known analytically as a function of r, but only numerically, the calculation of all quantities in this section was done numerically. A point nucleus was assumed throughout.

A. Bound-State Wave Functions and Potentials

A numerical RHFS program developed by Smith and Johnson,[17] and later by Feiock, was used. The program produces as output the numerical values of $g_{n\kappa}$ and $f_{n\kappa}$ for all occupied bound states, the binding energies of all such states, and the numerical values of three potential terms of Eq. (13). In all numerical work, the potential was parametrized in a Coulomb-like form

$$V(r)=-\alpha Z(r)/r\ , \qquad (36)$$

the function $Z(r)$ being monotonically decreasing with r and less rapidly varying for small r than $V(r)$.

B. Continuum-State Wave Functions

The integration of the continuum functions g_κ and f_κ was begun with a 10-point Lagrange integration scheme.[21] In order that the functions remain bounded near $r=0$, integration for small r was carried out for G_κ, F_κ defined by

$$g_\kappa(pr)=r^{\gamma-1}G_\kappa(pr)\ , \qquad f_\kappa(pr)=r^{\gamma-1}F_\kappa(pr)\ , \qquad (37)$$

with $\gamma=[\kappa^2-(\alpha Z)]^{1/2}$, with the result that Eqs. (9) take on the form

$$\frac{dG_\kappa}{dx}=-\frac{(\gamma+\kappa)G_\kappa}{x}-\left(\frac{(E+1)}{p}-\frac{\alpha Z(r)}{x}\right)F_\kappa\ ,$$
$$\frac{dF_\kappa}{dx}=-\frac{(\gamma-\kappa)F_\kappa}{x}+\left(\frac{(E-1)}{p}-\frac{\alpha Z(r)}{x}\right)G_\kappa\ , \qquad (38)$$

with $x=pr$, $Z(r)\ge 0$, and E in electron mass units. The potential in Eq. (38), $V(r)=+\alpha Z(r)/r$, is the sum of the nuclear-Coulomb and direct-interaction terms ($\alpha Z/r-V^D$) of Eq. (13). The exchange term $\overline{V}^E$ is omitted, since the incident positron has no exchange interaction with atomic electrons.

In order to begin the integration, the boundary values $G_{r=0}$, $F_{r=0}$, $(dG/dr)_{r=0}$, and $(dF/dr)_{r=0}$ were obtained from the standard power series expansion in r, since for a point nucleus the potential must be Coulomb-like at small r. Aside from normalizations, these values are given by

$$G(0)=1,\quad F(0)=-\alpha Z/(\gamma-\kappa),\quad \kappa<0$$
$$F(0)=1,\quad G(0)=\alpha Z/(\gamma+\kappa),\quad \kappa>0 \qquad (39)$$
$$G'(0)=[(E-1)\alpha ZG(0)-(E+1)(\gamma+1-\kappa)F(0)]/(2\gamma+1),$$
$$F'(0)=[\alpha Z(E+1)F(0)+(E-1)(\gamma+\kappa+1)G(0)]/(2\gamma+1)\ .$$

After the first few values of G_κ and F_κ were obtained, integration of g_κ and f_κ was continued using a ninth-order predict-correct scheme.

As a test of the accuracy of the starting scheme, the values obtained for a Coulomb potential for $Z=0$ and $Z=80$ were compared with those resulting from a series expansion for small r, and with the exact Coulomb wave functions. Differences in both cases were never found to be in excess of one part in 10^6, and nearly all differences were less than one part in 10^7. There is of course a further loss

of accuracy as the numerical wave functions are integrated outward from the starting points.

C. Phase Shifts and Normalizations

In contrast to previous work on SQA in which a pure Coulomb potential was assumed,[11] exact analytical expressions for the partial-wave phase shifts and the normalizations for g_κ and f_κ in Eq. (10) are not available in this work.

Numerical calculations of these quantities in non-Coulomb central potentials have been carried out by Matese and Johnson[13] and by Schmickley and Pratt[22] in studies of the atomic photoeffect, and by Lin, Sherman, and Percus[23] in studying elastic-electron scattering.

Phase shifts and normalizations were calculated in this work by parametrizing the functions f_κ, g_κ in a form similar to the asymptotic free-field limit in Eq. (12):

$$g_\kappa(pr) = \left(\frac{E+m}{2E}\right)^{1/2} C_\kappa(r)\cos\phi_\kappa(pr)/pr \ ,$$
$$f_\kappa(pr) = \left(\frac{E-m}{2E}\right)^{1/2} C_\kappa(r)\sin\phi_\kappa(pr)/pr \ , \tag{40}$$

with $\phi_\kappa(pr) = pr + \Delta_\kappa(r)$. In the limit as $pr \to \infty$ and $V(r) \to 0$, $C_\kappa(r) \to$ const, and $\Delta_\kappa(r) \to \delta'_\kappa - \frac{1}{2}(l+1)\pi$, provided $V(r) \to 0$ faster than $1/r$. δ'_κ is then the phase shift for the partial wave defined by κ, and $\delta'_\kappa = 0$ for zero scattering potential.

Substitution of Eq. (40) into Eq. (9) yields the following differential equations for ϕ_κ and C_κ:

$$\frac{d\phi_\kappa}{dr} - \frac{\kappa}{r}\sin 2\phi_\kappa + \frac{E}{p}V(r) + \frac{m}{p}V(r)\cos 2\phi_\kappa - p = 0 ,$$
$$\frac{dC_\kappa}{dr} + \left(\frac{\kappa}{r}\cos 2\phi_\kappa + \frac{m}{p}V(r)\sin 2\phi_\kappa\right) C_\kappa = 0 \ . \tag{41}$$

The integration of the first of Eqs. (41), involving only ϕ_κ, was begun by utilizing the parametrizations of Eq. (40):

$$\phi_\kappa(pr) = \tan^{-1}\left\{\left[\left(\frac{E+m}{E-m}\right)^{1/2}\right] f_\kappa/g_\kappa\right\} , \tag{42}$$

the values of f_κ and g_κ being determined by the starting Lagrange integration scheme.[21]

The determination of the asymptotic limit of $\Delta_\kappa(pr)$ was carried out by transforming $\phi_\kappa(pr)$ according to

$$\tan\phi_\kappa = \frac{1}{p}\left(\frac{\kappa}{r} + \frac{1}{t}\frac{dt}{dr}\right) , \tag{43}$$

so that, for large r where $V(r) = 0$, Eq. (41) yields the Ricatti-Bessel differential equation in $\xi = pr$:

$$\xi^2\frac{d^2t}{d\xi^2} + [\xi^2 - \kappa(\kappa+1)]t = 0 .$$

The solutions to this equation are[24]

$$t(\xi) = \xi[A_\kappa j_\kappa(\xi) + B_\kappa y_\kappa(\xi)] \ , \tag{44}$$

$j_\kappa(\xi)$ and $y_\kappa(\xi)$ being the spherical Bessel functions of the first and second kind, respectively. Then in a region of space for which $V(r) = 0$, the behavior of $\phi_\kappa(pr)$ is given by

$$\tan\phi_\kappa(pr) = -\frac{j_{\kappa-1}(pr) + A_\kappa y_{\kappa-1}(pr)}{j_\kappa(pr) + A_\kappa y_\kappa(pr)} \ . \tag{45}$$

Once the constant A_κ is determined by integrating $\phi_\kappa(pr)$ out to some r_0 sufficiently large that $V(r_0)$ can be taken to be zero, the asymptotic limit of $\Delta_\kappa(pr)$ is obtained from Eq. (45) and the asymptotic limits

$$j_l(x) \to (1/x)\sin(x - \tfrac{1}{2}l\pi), \qquad x \to \infty ,$$
$$y_l(x) \to -(1/x)\cos(x - \tfrac{1}{2}l\pi), \qquad x \to \infty \ . \tag{46}$$

Thus

$$\delta'_\kappa = \lim_{r\to\infty} \Delta_\kappa(pr) + \tfrac{1}{2}(l+1)\pi = \tan^{-1}A_\kappa(pr_0) . \tag{47}$$

The asymptotic limit of C_κ was obtained from Eq. (40), the asymptotic limit of g_κ and f_κ in Eq. (40) being determined by matching at r_0 with spherical Bessel functions and using Eq. (46). Since it can be shown that the asymptotic behavior of $\Delta_\kappa(pr)$ is given by[22] $\Delta_\kappa(pr) \to \kappa\cos(2pr)/pr + \text{const}$, $pr \to \infty$, the matching process for $\Delta_\kappa(pr_0)$ and $C_\kappa(pr_0)$ was carried out for several points on a cycle of $\cos(2pr)$, yielding an average over the cycle. Such an averaging was also carried out by Schmickley and Pratt[22] for phase shifts for the atomic photoeffect.

As a check on the accuracy of the technique, phase shifts and normalizations were calculated for $V(r) = 0$. It is expected that $\delta'_\kappa = 0$ and $C_\kappa = 1$ if $F_\kappa(0)$ and $G_\kappa(0)$ are normalized correctly. It was found that $|\delta'_\kappa| < 10^{-5}$ for $|\kappa| \leq 5$, $|\delta'_\kappa| < 10^{-4}$ for $|\kappa| \leq 20$, and that $|1 - C_\kappa| < 10^{-5}$ for $|\kappa| \leq 10$ and $|1 - C_\kappa| < 10^{-3}$ for $|\kappa| \leq 20$. Another check was made by comparison with the phase-shift values computed by Lin, Sherman, and Percus[23] for elastic electron scattering. Typical disagreements were less than their estimate of error.

From these and other considerations, it is felt that phase shifts computed by the present technique are accurate to one part in the fourth decimal place and normalizations to about three parts in 10^4.

D. Radial Integrals

Spherical Bessel functions in the integrals (20) were calculated using upward recurrence for $\omega r > l + \frac{1}{2}$ and downward recurrence for $\omega r < l + \frac{1}{2}$, according to the technique of Miller.[25] Integration was carried out using an eleventh-order, closed-type Newton-Cotes formula.[26] Integrals for a

typical atom were evaluated for step size of $\pi/20\omega$. The worst relative differences resulting from doubling step size were 0.04%.

Considering the various sources of error, relative errors in the integrals (20) for step sizes used are felt to be no worse than 0.1%, most of the error being due to normalization constants.

IV. RESULTS

A. Total Cross Sections

K-shell total cross sections calculated by the present method, using RHFS central potentials, are listed in Table I, with a comparison with the cross sections of Johnson *et al.*[9] for a pure Coulomb potential. The unscreened values for $Z=80$ were computed using the methods of Sec. III.[27] As a test of the accuracy of the method, unscreened differential and total cross sections for $Z=79$ and $E=1.5mc^2$ were computed and compared with Johnson's values,[11] with agreement to at least five decimal places. Screening increases the SQA K-shell total cross sections by several percent for all energies and atomic numbers considered. For a given energy, screening corrections to the cross sections increase with increasing atomic number, the corrections for $E=1.5mc^2$ varying from about 2% for $Z=47$ to about 8% for $Z=90$. Screening effects are also most pronounced for low energy, for $Z=82$ the corrections ranging from 3% for $E=1.75mc^2$ to 23% for $E=1.25mc^2$.

The relative importance of screening on L-shell cross sections is indicated in Table II for $Z=80$. The Coulomb cross sections listed were computed by the methods of Sec. III.[28] Screening increases the L-shell cross sections for $E=1.25mc^2$ to a smaller degree than for the K shell, and actually decreases them for $E=1.5mc^2$.

Table III lists the screened total cross sections for the three L shells of several atoms. If σ_L is defined as $\sigma_L=\sigma_{L_I}+\sigma_{L_{II}}+\sigma_{L_{III}}$, it can be seen that σ_L/σ_K is a non-negligible ratio that increases with increasing Z, is practically energy independent for the range considered, and varies from about 0.13 for $Z=47$ to 0.22 for $Z=90$. The value for lead, $Z=82$, is about 0.20, somewhat higher than the value 0.16 predicted by Bethe[6] using the Born approximation.

Also compared in Table III is the quantity $\sigma_K+\sigma_{L_I}$, calculated here with screening, with the corresponding unscreened value of Sheth and Swamy.[10] The screened values are nearly all larger than the unscreened values, the difference being largest for high Z and low positron energy. Unfortunately, for purposes of comparison, Sheth and Swamy give cross sections for only the L_I shell, although, as the screened values indicate, the L_{II}-shell contribution is of the same order of magnitude as the L_I, at least for high-Z elements. The smallness of the L_{III} cross section for high Z, as compared to the L_I and L_{II} values, can be attributed to the relative smallness of the L_{III} radial functions g_{κ_B} and f_{κ_B}, in the region of small r, compared to the functions for the L_{II} shell. For small r, g_{κ_B} and f_{κ_B} behave in a Coulomb potential as $r^{\gamma-1}$, with $\gamma=[\kappa^2-(\alpha Z)^2]^{1/2}$. For $Z=82$, $\gamma=0.80$ for the L_I and L_{II} shells, and $\gamma=1.91$ for the L_{III} shell.

TABLE I. Screened and unscreened K-shell total cross sections in barns. (a) Results of present calculation. (b) Values for pure Coulomb potential. Coulomb cross sections for $Z=47$, 73, 82, and 90 are from Johnson *et al.* (Ref. 9).

	$E=1.25mc^2$		$E=1.50mc^2$		$E=1.75mc^2$	
Z	(a)	(b)	(a)	(b)	(a)	(b)
47	0.0477	0.0450	0.0481	0.0472	0.0446	0.0442
73	0.369	0.315	0.427	0.407	0.385	0.376
80	0.546	0.449	0.669	0.632	0.611	0.595
82	0.605	0.492	0.755	0.710	0.693	0.673
90	0.879	0.682	1.182	1.095	1.107	1.069

TABLE II. Screened and unscreened L-shell total cross sections in millibarns for $Z=80$. (a) Screened values from the present calculation. (b) Values for unscreened Coulomb potential.

	L_I		L_{II}		L_{III}	
$E(mc^2)$	(a)	(b)	(a)	(b)	(a)	(b)
1.25	78.7	72.5	23.1	22.5	1.65	1.64
1.50	96.0	102.6	29.7	33.2	2.87	3.24

B. Differential Cross Sections

Differential cross sections for unpolarized positron and photon beams $(d\sigma/d\Omega)_{\text{unpol}}$ are plotted in

TABLE III. L-shell total cross sections in millibarns. (a), (b), and (c) screened values by present calculation for L_I, L_{II}, L_{III}, respectively. (d) $\sigma_K+\sigma_{L_I}$ by present method. (e) $\sigma_K+\sigma_{L_I}$ according to Sheth and Swamy (Ref. 10). (f) $\sigma_K+\sigma_{L_I}+\sigma_{L_{II}}+\sigma_{L_{III}}$ by present method. Energies are in units of mc^2.

E	Z	(a)	(b)	(c)	(d)	(e)	(f)
1.25	47	5.51	0.652	0.107	53.2	51.3	54.0
	73	51.0	12.5	0.999	420	364	434
	82	88.3	27.4	1.90	693	572	723
	90	134.2	51.8	3.24	1013	797	1068
1.50	47	5.43	0.601	0.175	53.5	53.6	54.3
	73	58.4	14.9	1.763	485	470	502
	82	109.8	35.8	3.29	865	825	904
	90	180.8	73.4	5.51	1363	1280	1442
1.75	47	4.95	0.504	0.207	49.6	50.1	50.3
	73	51.9	13.7	2.17	437	434	453
	82	99.6	33.9	3.99	793	781	830
	90	168.3	71.5	6.54	1275	1249	1353

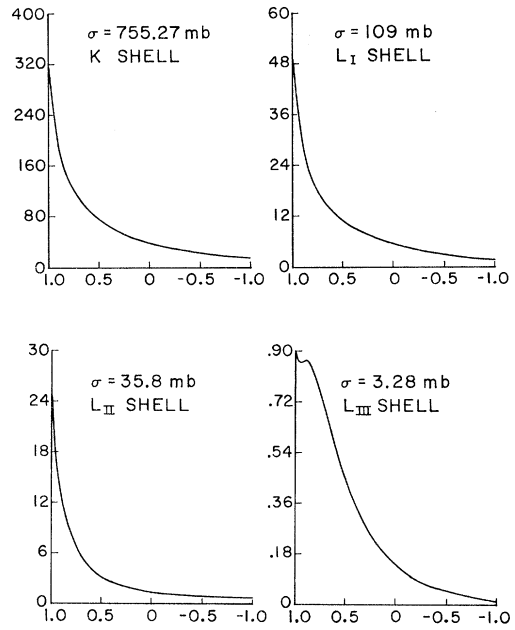

FIG. 1. Differential cross sections for SQA on Pb ($Z=82$) at incident positron energy $E=1.5mc^2$. $d\sigma/d\Omega$ in mb/sr is plotted against $\cos\theta$.

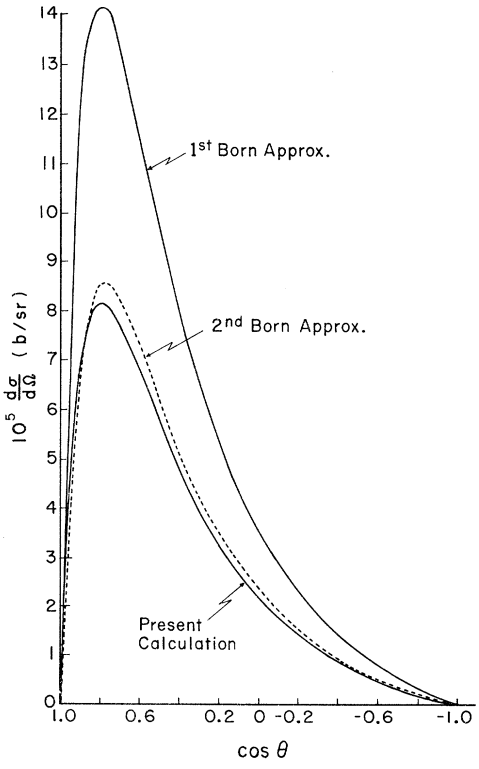

FIG. 2. K-shell differential cross section for $Z=10$, $E=1.5mc^2$. A comparison of the first and second Born approximations with the present calculation.

Fig. 1 for $Z=82$ and $E=1.5mc^2$. The angle between positron and photon momentum directions is denoted by θ. The angular distributions for the K, $L_{\rm I}$, and $L_{\rm II}$ shells peak sharply in the forward direction, in agreement with other recent predictions for the K shell in a Coulomb potential.

Figure 2 compares the K-shell angular distributions calculated by the present methods for $Z=10$, $E=1.5mc^2$ with the first Born-approximation results and the predictions of the recent second-order Born approximation by Moroi *et al.*[29] The maximum occurs away from the forward direction for this low-Z atom, in sharp contrast to K-shell annihilation in high-Z atoms, and in agreement in shape with the predictions of the first- and second-order Born approximations. The results of the present method agree fairly well with Moroi's predictions for most angles, as is to be expected (since screening effects should be small for such low Z and the smallness of αZ should make the Moroi expansion a reasonably good approximation). At extreme forward and backward angles, however, the Moroi prediction is several orders of magnitude smaller than the present prediction (1.97 μb/sr versus 1.34 μb/sr for $\theta=0$).

An interesting characteristic of the screened differential cross sections is the shift of the maximum away from the forward direction for the $L_{\rm III}$ shells for low Z for all energies. Apparently, this shift is characteristic of atoms of low Z or of subshells having low electron charge densities near the nuclear region (e.g., the $L_{\rm III}$ subshell). The

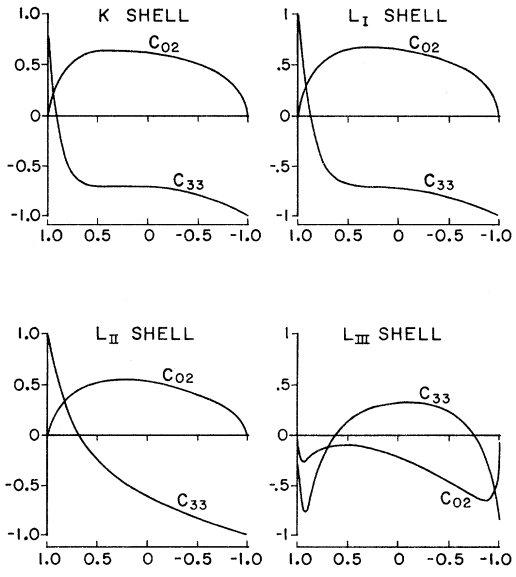

FIG. 3. Polarization correlations C_{02} and C_{33} for $Z=82$ at $E=1.5mc^2$. The normalized correlation functions are plotted against $\cos\theta$ for the K, $L_{\rm I}$, $L_{\rm II}$, and $L_{\rm III}$ shells.

shift can be expected to be more obvious for higher M-shell angular distributions.

C. Polarization Correlations

The two polarization correlation functions of particular interest in this work, C_{02} and C_{33}, are plotted in Fig. 3 for $Z=82$ and $E=1.5mc^2$.[28]

The function $C_{02}(\theta)$ correlates the azimuthal asymmetry of an unpolarized emitted photon beam, the azimuthal angle being measured from the plane formed by the positron and photon momenta, to the polarization of an incoming positron beam in a direction perpendicular to this plane. The function C_{02} vanishes at both forward and backward directions, as is to be expected from the structure of the amplitudes $G_{\pm}$, $F_{\pm}$ for the K and L shells. It is noteworthy that for the L_{III} shell for $Z=82$ the function C_{02} is of opposite sign to that for the K, L_I, and L_{II} shells.

It is seen that for the K, L_I, and L_{II} shells the function C_{33} is always $+1$ in the forward direction, -1 in the backward direction, as expected from the form of $G_{\pm}$, $F_{\pm}$. Thus, photons emitted at $\theta=0°$ by annihilation in one of those shells will have the same helicity as that of a longitudinally polarized incident positron beam (photons emitted at $\theta=180°$ will have opposite helicity). Thus, SQA could be of considerable experimental interest, insofar as it could constitute a method for obtaining circularly polarized photon beams from polarized positron beams. Particularly useful would be the complete correlation in the forward direction, where the differential cross section is sharply spiked for heavy atoms, especially for higher positron energies, and the fact that the cross sections for these three shells could be expected to be the main contribution to the over-all atomic cross section.

The complete correlation for C_{33} in the forward direction does not exist for L_{III}-shell annihilation, owing to the fact that the functions B_{ij} [Eq. (33)] are actually summed over $m_B=\frac{1}{2}$ and $m_B=\frac{3}{2}$. The function for this shell is of the form

$$C_{33}=\frac{(B_{33})_{m_B=1/2}+(B_{33})_{m_B=3/2}}{(B_{00})_{m_B=1/2}+(B_{00})_{m_B=3/2}}\ .$$

Pratt[30] has demonstrated that in processes involving high-energy photons and positrons, the probability for the outgoing photon, when emitted in the forward direction to have helicity opposite to that of the incoming positron is reduced by a factor $1/E$ (E is the incident positron energy) compared to the probability for the photon having the same helicity as the positron, regardless of the bound state. Thus, as $E\to\infty$, the correlation should become complete in the forward direction. This tendency was observed in the numerical results.

ACKNOWLEDGMENTS

The authors would like to thank Dr. Frank Smith and Dr. Frank Feiock for their work on the numerical RHFS program used in this work. Also, many helpful discussions with Dr. Anthony Desiderio are acknowledged.

---

*Research supported in part by the U. S. Atomic Energy Commission under Contract No. AT(11-1)-427.

†Work based in part on a dissertation submitted by K. W. B. in partial fulfillment of the requirements for the Ph. D. degree at the University of Notre Dame.

‡Present address: Canisius College, Buffalo, N. Y. 14208.

[1]S. Meric, Rev. Fac. Sci. Univ. Istanbul 15A, 179 (1950); also, Istanbul Univ. Fen Fak. Mecmuasi A15, 136 (1950). Abstracts available in Nucl. Sci. Abstr. V, 965 (1951) and Sci. Abstr. A53, 1030 (1950).

[2]L. Sodickson, W. Bowman, J. Stephenson, and R. Weinstein, Phys. Rev. 124, 1851 (1961).

[3]H. Langhoff, H. Weigmann, and A. Flammersfeld, Nucl. Phys. 41, 575 (1963).

[4]H. Weigmann, H. Hansen, and A. Flammersfeld, Nucl. Phys. 45, 555 (1963).

[5]E. Fermi and G. E. Uhlenbeck, Phys. Rev. 44, 510 (1933).

[6]H. A. Bethe, Proc. Roy. Soc. (London) 150, 136 (1935).

[7]J. C. Jaeger and H. R. Hulme, Proc. Cambridge Phil. Soc. 32, 158 (1936).

[8]H. J. Bhabha and H. R. Hulme, Proc. Roy. Soc. (London) A146, 723 (1934).

[9]W. R. Johnson, D. J. Buss, and C. O. Carroll, Phys. Rev. 135, A1232 (1964).

[10]C. V. Sheth and N. V. V. J. Swamy, Phys. Rev. 167, 319 (1968).

[11]W. R. Johnson, Phys. Rev. 159, 61 (1967).

[12]W. R. Alling and W. R. Johnson, Phys. Rev. 139, 4A (1965).

[13]J. J. Matese and W. R. Johnson, Phys. Rev. 140, 1A (1965); G. Rakavy and A. Ron, Phys. Letters 19, 207 (1965); Phys. Rev. 159, 50 (1967).

[14]R. H. Pratt, R. D. Levee, R. L. Pexton, and W. Aron, Phys. Rev. 134, A898 (1964).

[15]M. E. Rose, *Elementary Theory of Angular Momentum* (Wiley, New York, 1957).

[16]J. J. Sakurai, *Advanced Quantum Mechanics* (Addison-Wesley, New York, 1968), pp. 140–143.

[17]F. C. Smith and W. R. Johnson, Phys. Rev. 160, 136 (1967).

[18]D. Liberman, J. T. Waber, and D. T. Cromer, Phys. Rev. 137, A27 (1965).

[19]J. C. Slater, Phys. Rev. 81, 3 (1951).

[20]A. I. Akhiezer and V. B. Berestetskii, *Quantum Electrodynamics* (Interscience, New York, 1965).

[21]*Handbook of Mathematical Functions*, edited by M. Abramowitz (National Bureau of Standards, Washington, D. C., 1968), Vol. 55, p. 878, 915.

[22]R. D. Schmickley and R. H. Pratt, Phys. Rev. 164,

104 (1967).
[23]S. R. Lin, N. Sherman, and J. K. Percus, Nucl. Phys. 45, 492 (1963).
[24]Reference 21, p. 445.
[25]Reference 21, Chap. 10.
[26]Reference 21, p. 886, Eq. 25.4.18.
[27]In calculating Coulomb cross sections, bound-state wave functions, and continuum phase shifts and normalizations were evaluated analytically, rather than numerically.
[28]Tables of differential cross sections and polarization correlations for K and L shell SQA for $Z=47$, 73, 80, 82, 90 and energies $E=1.25$, 1.5, and $1.75mc^2$ are available.
[29]D. S. Moroi, A. Davidz, and R. F. Kess, Phys. Rev. 1, 1647 (1970).
[30]R. H. Pratt, Phys. Rev. 123, 1508 (1961).

PHYSICAL REVIEW A VOLUME 6, NUMBER 5 NOVEMBER 1972

Quadrupole Shielding and Antishielding Factors for Several Atomic Ground States*

R. M. Sternheimer
Brookhaven National Laboratory, Upton, New York 11973
(Received 19 May 1972)

The atomic shielding or antishielding factor R for the quadrupole hyperfine structure has been obtained for seven atomic ground states ranging from F $2p^5$ to Br $4p^5$. The values of R were determined by means of the perturbed wave functions $v_1(nl \rightarrow l')$, as obtained by solving the inhomogeneous Schrödinger equation for each type of excitation of the core electrons by the nuclear quadrupole moment Q. The resulting values of R have been listed, together with those for four atomic states which had been previously investigated. For the atomic ground states in this region of the Periodic Table, R is generally positive (shielding), and of the order of +0.1, except for Al $3p$ and Ga $4p$, for which R is negative, because of the antishielding provided by the $2p \rightarrow p$ and $3p \rightarrow p$ perturbations, respectively. The resulting correction factors $C = 1/(1-R)$ have been applied to the quadrupole moments of 11 nuclear isotopes. We have also obtained the ionic antishielding factor γ_∞ for the Sc^{3+} ion, $\gamma_\infty(Sc^{3+}) \cong -11.2$.

I. INTRODUCTION

The purpose of the present paper is to give the results of calculations of the quadrupole shielding (or antishielding) factor[1] R for several atomic ground states, ranging from B $2p$ to Br $4p^5$. Altogether results will be presented for eleven atomic states in this region of the Periodic Table. The results for four of these states have been obtained previously,[2,3] namely, for B $2p$, Al $3p$, Cu $3d^9 4s^2$, and Cu $3d^{10}4p$. For the seven additional states, the present calculations are new; these states consist of O $2p^4$, F $2p^5$, Cl $3p^5$, Sc $3d$, Fe^{2+} $3d^6$, Ga $4p$, and Br $4p^5$. The method of the calculations is entirely similar to that which has been used in previous papers.[1-5] In particular, we used the computer programs which have been described in Ref. 2.

The final results for the values of R and of the resulting quadrupole moment correction factor $C = 1/(1-R)$ are given in Table VIII. In Sec. II, we shall describe the calculations of R and of the associated ionic antishielding factors[6] γ_∞. The individual terms of R and γ_∞ for each case are presented in Tables I–VII. We shall also discuss the present results for R, and in particular, the decrease of R (i.e., decrease of shielding) with increasing atomic number Z for the case of the halogen-atom ground states.

In Sec. III, we apply the correction factors C to the experimental quadrupole moments Q_{expt} of eight nuclei to obtain corrected values Q_{corr}. We note that, in addition, Q_{corr} values have been previously obtained: (a) for three nuclei, namely, Al^{27}, Cu^{63}, and Cu^{65} in Refs. 2 and 3, and (b) for 12 alkali isotopes from hfs measurements in the excited np states (see Ref. 4). In Sec. III of the present paper, the determination of the presently obtained Q_{corr} values has been combined with that of $Q(Al^{27})$, $Q(Cu^{63})$, and $Q(Cu^{65})$, and the results have been presented in Table IX, which thus gives the values of Q_{corr} for 11 nuclei.

Finally, in Sec. IV we give a brief summary and general discussion of the present results.

II. CALCULATIONS OF R

As already mentioned in the Introduction, the calculations of R follow the same lines as in the work of Refs. 1–5. For the unperturbed wave functions of the core electrons u_0', we used in all cases the Hartree–Fock wave functions obtained by Clementi.[7] The effective potential $V_{0,HF}$ corresponding to these wave functions was obtained by the procedure previously introduced by the author,[5] namely,

$$V_{0,HF} - E_{0,HF} = \frac{1}{u_0'} \frac{d^2u_0'}{dr^2} - \frac{l(l+1)}{r^2}, \qquad (1)$$

where $E_{0,HF}$ is the effective Hartree-Fock energy eigenvalue and l is the azimuthal quantum number